Research Article

20(S)-ginsenoside Rh2 ameliorates ATRA resistance in APL by modulating lactylation-driven METTL3

Siyu Cheng [a], Langqun Chen [a], Jiahui Ying [a], Ying Wang [a], Wenjuan Jiang [a], Qi Zhang [a], Hong Zhang [a], Jiahe Wang [a], Chen Wang [a], Huimin Wu [a], Jing Ye [a,b,**], Liang Zhang [a,*]

[a] Jiangsu Key Laboratory for Pharmacology and Safety Evaluation of Chinese Materia Medica, School of Pharmacy, Nanjing University of Chinese Medicine, Nanjing, Jiangsu, China
[b] State Key Laboratory of Pharmaceutical Biotechnology, School of Life Sciences, Nanjing University, Nanjing, Jiangsu, China

ABSTRACT

Background: 20(S)-ginsenoside Rh2(GRh2), an effective natural histone deacetylase inhibitor, can inhibit acute myeloid leukemia (AML) cell proliferation. Lactate regulated histone lactylation, which has different temporal dynamics from acetylation. However, whether the high level of lactylation modification that we first detected in acute promyelocytic leukemia (APL) is associated with all-trans retinoic acid (ATRA) resistance has not been reported. Furthermore, Whether GRh2 can regulate lactylation modification in ATRA-resistant APL remains unknown.
Methods: Lactylation and METTL3 expression levels in ATRA-sensitive and ATRA-resistant APL cells were detected by Western blot analysis, qRT-PCR and CO-IP. Flow cytometry (FCM) and APL xenograft mouse models were used to determine the effect of METTL3 and GRh2 on ATRA-resistance.
Results: Histone lactylation and METTL3 expression levels were considerably upregulated in ATRA-resistant APL cells. METTL3 was regulated by histone lactylation and direct lactylation modification. Overexpression of METTL3 promoted ATRA-resistance. GRh2 ameliorated ATRA-resistance by downregulated lactylation level and directly inhibiting METTL3.
Conclusions: This study suggests that lactylation-modified METTL3 could provide a promising strategy for ameliorating ATRA-resistance in APL, and GRh2 could act as a potential lactylation-modified METTL3 inhibitor to ameliorate ATRA-resistance in APL.

1. Introduction

Acute promyelocytic leukemia (APL), known as the M3 type of Acute myeloid leukemia (AML), accounts for about 10–15 % of AML [1]. In the mid-1980s, the differentiation treatment with all-trans retinoic acid (ATRA) considerably improved the remission and survival rates of clinical APL patients [2]. However, 10–30 % of APL patients still exhibit primary or secondary resistance to ATRA, limiting its therapeutic efficacy and clinical application [3]. Therefore, exploring the potential mechanisms of ATRA-resistance and developing new therapeutic targets are crucial for improving the prognosis of APL patients.

Clinical evidence has suggested that the occurrence of early deaths in APL patients treated with ATRA is associated with higher lactate dehydrogenase (LDH) levels [4]. During glycolysis, LDH is a key metabolic enzyme for the production of lactate [5]. The high concentration of LDH promoted lactate production and histone lactylation. Lactate regulated histone lactylation, which has different temporal dynamics from acetylation [6]. Targeting histone deacetylase in ATRA-resistant APL promotes leukemia cell differentiation and apoptosis [7]. K.Noack et al. found that there is an interaction between histone deacetylase and ATRA in APL [8]. However, whether the high level of lactylation modification that we first detected in APL is associated with ATRA resistance has not been reported.

Our team has shown that GRh2 induces apoptosis in APL cells [9]. Moreover, Liu et al. reported GRh2 as an effective natural histone deacetylase inhibitor, inhibiting CML and M3 type of AML cells

proliferation [10]. However, whether GRh2 can regulate lactylation modification in ATRA-resistant APL remains unknown.

2. Materials and methods

2.1. Cell culture and transfection

NB4, was acquired from the North China Biotechnology Research Institute (BNCC341933). NB4-R1 and NB4-R2, were donated by the Hematology Research Institute of Ruijin Hospital affiliated with Shanghai Jiao Tong University School of Medicine. NB4-R1 are from patients with secondary ATRA resistance, while the resistance of NB4-R2 is related to mutations in the ligand-binding portion of the intracellular PML-RARα fusion protein. APL cells were cultured in RPMI 1640 (KGM31800-500, KeyGEN BioTECH, China) with 15 % fetal bovine serum (AB-FBS0500S, ABW, USA).

An si-METTL3 1 (5′-GCUGCACUUCAGACGAAUUTT-3′); an si-METTL3 2 (5′- GCUCAACAUACCCGUACUATT-3′); an si-METTL3 3 (5′-GCAAGAAUUCUGUGAC.

UAUTT-3') were established by KeyGEN BioTECH (China). The transfection experiments were performed by RFectSP siRNA transfection reagent (11024, biodai, China). LV-METTL3-OE lentivirus was established by KeyGEN BioTECH (China). The transfection experiments were performed by RFectSP plasmid transfection reagent (#21027, biodai, China).

2.2. Reagents and drugs

ATRA (purity = 99.74 %, HY-14649), Oxamate (purity = 99.72 %, HY-W013032A), and Lactate (purity = 91.61 %, HY-B2227) were purchased from MCE Limited (USA). GRh2 (purity = 95 %, 78214-33-2) was acquired from Nantong Feiyu Biotechnology (China). Nitro Tetrazolium Blue (NBT) (#298-83-9) was sourced from Sigma-Aldrich (USA).

The antibodies used included: Anti-L-Lactyl Lysine Rabbit pAb (PTM-1401) and Anti-Acetyllysine Mouse mAb (PTM-101) obtained from PTMBIO (China). Lactic acid-Histone H3–K18 Rabbit mAb (A21214) and H3 Rabbit mAb (A17562) were purchased from ABclonal Technology (China).METTL3 Polyclonal antibody (15073-1-AP), lamin B1 Polyclonal antibody (12987-1-AP),Beta Actin Monoclonal antibody (66009-1-lg), HRP-conjugated Affinipure Goat Anti-Mouse IgG(H + L) (SA00001-1), and HRP-conjugated Affinipure Goat Anti-Rabbit IgG(H + L) (SA00001-1) were sourced from Proteintech (USA).

2.3. Quantification of lactate dehydrogenase and lactate

Using the Lactate Dehydrogenase Assay Kit (A020-2-1, Nanjing Jiancheng Bioengineering Institute, China), LDH levels were determined via microplate method, as per the instructions. Lactic Acid levels were quantified using the Lactic Acid Assay Kit (A019-2-1, Nanjing Jiancheng Bioengineering Institute, China) according to the colorimetric method provided in the manual.

2.4. RNA-seq and KEGG analysis

APL cells (1×10^6 cells/mL) were seeded in 100 mm culture dishes and subjected to respective treatments. APL cells were harvested, and total RNA extracted. The RNA concentration and purity were determined using Nanodrop2000. mRNA was isolated from total RNA using magnetic beads with Oligo(dT) for A-T base pairing. Short sequence fragments were sequenced using the Illumina Novaseq 6000 platform. The mRNA was randomly fragmented by adding fragmentation buffer, and fragments around 300bp were isolated using magnetic beads. Under the action of reverse transcriptase, with the addition of six-base random primers, a stable double-stranded structure was formed from the mRNA template. Sequencing was performed on the Illumina platform.

2.5. Nitro tetrazolium blue reduction

APL cells (1×10^6 cells/mL) were seeded in 100 mm culture dishes and subjected to respective treatments. APL cells were harvested and 100 μL of the cell suspension was added to a 96-well plate, followed by 10 μL of Cell Counting Kit-8 (FD3788, Fude, China). Incubating at 37 °C for 2 h later, the remaining cell suspension was treated with NBT for 1 h. The ratio of NBT positive cells was measured at OD570/OD450.

2.6. Flow cytometry (FCM)

2.6.1. Detection of CD11b differentiation level
APL cells (1×10^6 cells/mL) were seeded in 100 mm culture dishes and subjected to respective treatments. Cells were collected and each test tube was added with PE-*anti*-human CD11b (982606, Biolegend, USA). Incubating in the dark at room-temperature for 30 min later, analysis was done using a flow cytometer (Accuri C6, BD Biosciences).

2.6.2. Detection of apoptotic rate in APL stem cells
APL cells (1×10^6 cells/mL) were seeded in 100 mm culture dishes and subjected to respective treatments. Cells were harvested and each test tube was added with PE-*anti*-humanCD34 (343505, Biolegend, USA), PE-cyanine 7 anti-human CD38 (303515, Biolegend, USA), and APC anti-human CD123 (306011, Biolegend, USA). Incubating in the dark at room-temperature for 20 min later, cells were washed once with PBS. After resuspending cells in 100 μl Binding Buffer, FITC Annexin V (640905, Biolegend, USA) was added and incubated in the dark at room-temperature for 15 min, followed by 7-AAD Viability Solution (420403, Biolegend, USA) and incubated for 5 min. Analysis was done using a flow cytometer (Accuri C6, BD Biosciences). Apoptosis of LSCs in population cells rate = LSCs apoptosis (CD34$^+$CD38$^-$CD123$^+$AnnexinV$^+$) amount of cells/number of LSCs before apoptosis.

2.6.3. Detection of APL leukemic burden
APL cells (1×10^6 cells/mL) were seeded in 100 mm culture dishes and subjected to respective treatments. Cells were harvested and each test tube was added with FITC-*anti*-mouse CD45 (157213, Biolegend, USA). Incubating in the dark at room-temperature for 30 min later, analysis was done using a flow cytometer (Accuri C6, BD Biosciences).

2.7. Western blot

APL cells (1×10^6 cells/mL) were seeded in 100 mm culture dishes and subjected to respective treatments. Cells were collected, and total proteins were extracted using RIPA lysis buffer (P0013C, beyotime, China) or nuclear proteins were extracted using the Nuclear Protein Extraction Kit (AKPR022-2, Boxbio, China). Proteins were transferred to the PVDF membrane (88518, Invitrogen, USA) after electrophoresis. The PVDF membranes were incubated overnight with the primary antibodies in a refrigerator at 4 °C, followed incubation with the secondary antibodies at room-temperature for 1h. They were then visualized using a gel imaging system (Bio-Rad, USA).

2.8. Quantitative reverse transcription-polymerase chain reaction (qRT-PCR)

APL cells (1×10^6 cells/mL) were seeded in 100 mm culture dishes and subjected to respective treatments. Withing TRIzol reagent (#15596026, Invitrogen, USA), total RNA of APL cells was extracted. The total RNA was then reverse-transcribed into cDNA using the
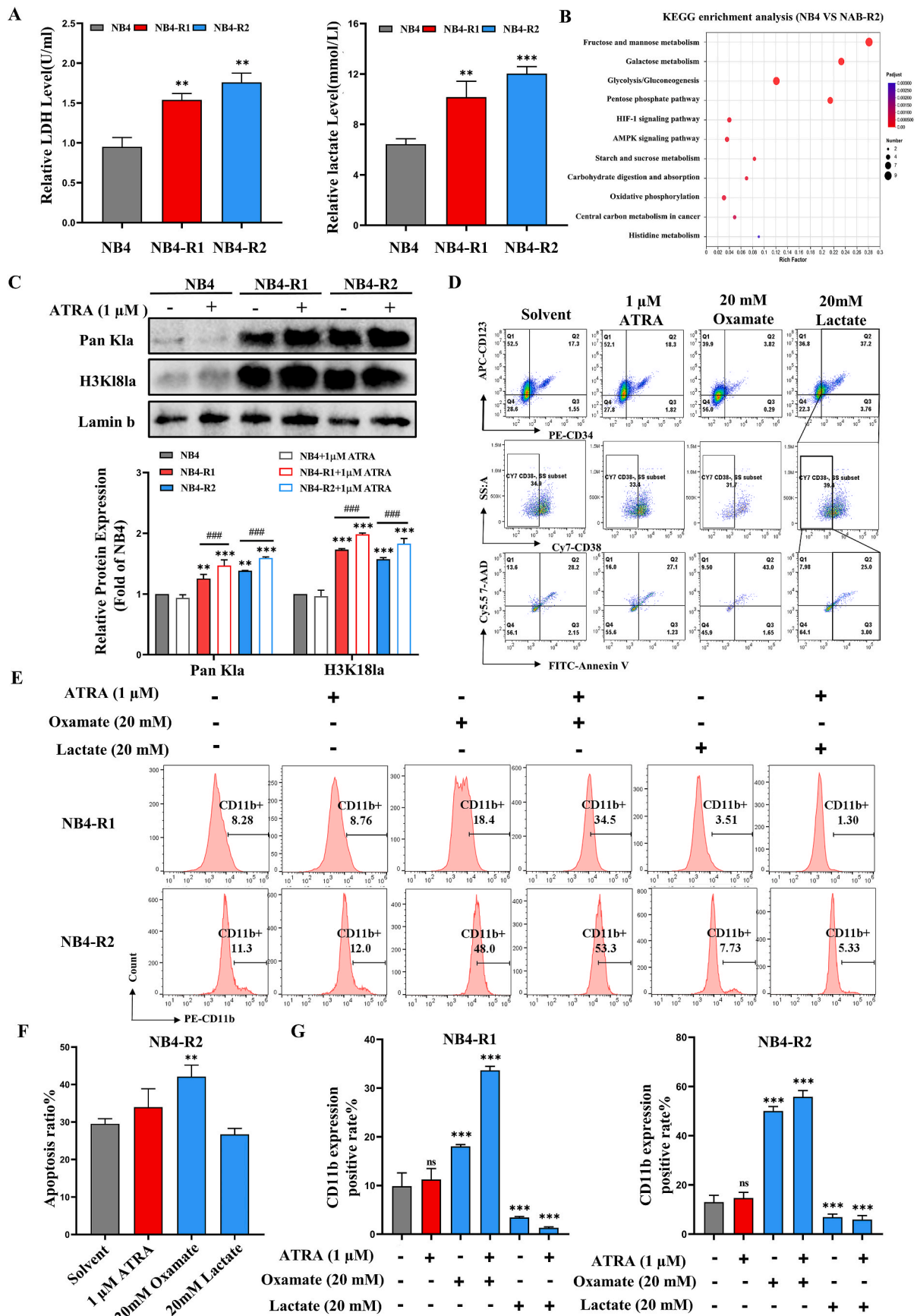
(caption on next page)

Fig. 1. Histone lactylation levels increased in ATRA-resistance APL cells

(A) LDH and Lactate assay kit to measure LDH and lactate levels in NB4-R2. (n = 6, **P < 0.01, ***P < 0.001 versus NB4). (B) KEGG analysis showing genes involved in Lactic acid metabolism pathway between NB4 and NB4-R2. (C) Detection of Pan Kla and H3K18la expression levels in NB4, NB4-R1 and NB4-R2 cells treated with 1 μM ATRA for 48 h by Western blot analysis. (n = 3, **P < 0.01, ***P < 0.001 versus NB4; ###P < 0.001). (D, F) The apoptosis rate of ATRA-resistance LSCs labeled with CD34$^+$CD38$^-$CD123$^+$ in NB4-R2 cell were treated with 20 μM oxamate or 20 μM lactate or 1 μM ATRA for 48 h was detected by FCM. (n = 3, **P < 0.01 versus solvent). (E, G) FCM were used to detect CD11b$^+$ cell ratios in NB4-R1 and NB4-R2 cells treated with 20 μM oxamate, 20 μM lactate, and 1 μM ATRA for 48 h (n = 3, ***P < 0.001).

HiScript II Q RT SuperMix for qPCR (+gDNA wiper) (R223-01, Vazyme, China). qRT-PCR was performed to detect mRNA expression levels using the ChamQ Universal SYBR qPCR Master Mix (Q711-02, Vazyme, China). β-actin was used as an internal control.

Primers for qRT-PCR are as follows.

Gene name	Primer sequences
METTL3	F: 5′- CTGTGTCCATCTGTCTTGCCATCTC-3′
	R: 5′-ACCTCGCTTTACCTCAATCAACTCC-3′
METTL14	F: 5′-AATCGCCTCCTCCCAAATCTAAATC-3′
	R: 5′-GTTCCACCTCTTCCTCCACCTC-3
YTHDF1	F: 5′-TGGACATTGGCACCTGGGATAAC-3′
	R: 5′-TGGACATTGGCACCTGGGATAAC-3′
YTHDF2	F: 5′- GCCATTGCCTCCACCTCCAC-3′
	R: 5′-GTAGATCCAGAACCAGCCTGAGAC-3′
YTHDC1	F: 5′- GCAAGCAGATCCAGCCAGTCTTC-3′
	R: 5′-TCCACTCCTTCCTCCTCATTCTCAG-3′
CD34	F: 5′- AGTTTGCTGCCTTCTGGGTTCATG-3′
	R:5′-ATGTTCCCTGGGTAGGTAACTCTGG-3′
CD38	F: 5′- GTTGGGAACTCAGACCGTACCTTG-3′
	R: 5′-CCGCTGGACCTGTGTGAACTG-3′
CD123	F: 5′- CCCGCATCCCTCACATGAAAGAC-3′
	R: 5′-TTCAGTCACCAGACACTCCTCCAG-3′
β-actin	F: 5′- GGCCAACCGCGAGAAGATGAC-3′
	R: 5′-GGATAGCACAGCCTGGATAGCAAC-3′

2.9. Co-immunoprecipitation (CO-IP)

APL cells (1 × 10^6 cells/mL) were seeded in 100 mm culture dishes and subjected to respective treatments. After collecting the cells, they were lysed in pre-cooled protein lysis buffer containing protease and phosphatase inhibitors. After thorough lysis, the samples were centrifuged to collect the supernatant, with 20 μL reserved as the Input. The remaining sample was divided into two parts: one for the IgG group and the other for the IP group. Each part was incubated with 1 μg of either IgG or the target antibody at 4 °C overnight. The next day, Protein A beads were added, and the mixture was rotated at 4 °C for 4 h. After washing three times with pre-cooled PBS, the beads were resuspended in an appropriate amount of PBS. The 5 × SDS sample buffer was added in a 4:1 ratio, boiled for 10 min at 100 °C, and subjected to Western Blot analysis.

2.10. N^6-methyladenosine(m^{6}A) methyltransferase activity assay

The Epigenase™ m^{6}A Methylase Activity/Inhibition Assay Kit (#P-9019, EpigenTek, USA) was used to specifically measure the catalytic activity of total m^{6}A methyltransferases. The methylated m^{6}A in the substrate can be recognized by a high affinity m^{6}A antibody. The proportion or amount of methylated m^{6}A is directly proportional to enzyme activity. Readings were taken at 450 nm using a spectrophotometer, and the methyltransferase activity was calculated according to the instructions provided with the kit.

2.11. In vivo experiments

The experiments were approved by the Experimental Ethics Committee of Nanjing University of Chinese Medicine (NO: 202304A019). All animal research was conducted according to the guidelines of the institutional animal ethics committee. When the tumor size and overall health condition met the euthanasia criteria, the animals were euthanized.

2.11.1. Orthotopic xenograft APL model

To establish the orthotopic xenograft APL model, NB4 cells (5 × 10^6) transduced with METTL3-overexpressing lentivirus were injected into the tail vein of the male BALB/C nude mice (GemPharmatech, China) at 4-5-week-old. Starting from day 11, 20 mg/kg ATRA was injected intraperitoneally every alternate day. After 20 days of treatment, the mice were euthanized. The APL burden in mouse bone marrow cells was determined using the Wright-Giemsa staining method and FCM analysis of CD45 positive cells.

2.11.2. Subcutaneous xenograft APL model

To establish the subcutaneous xenograft APL model, NB4 cells (5 × 10^6) transduced with METTL3-overexpressing lentivirus were subcutaneously injected into the male BALB/C nude mice (GemPharmatech, China) at 4-5-week-old. 20 mg/kg ATRA was injected intraperitoneally every alternate day when the tumor volume reached approximately 100–200 mm^3. After 20 days of treatment, the mice were euthanized. The spleen was examined using H&E staining to detect APL cell infiltration. The tumor was assessed using IHC to detect METTL3 expression, with tumor volume calculated as $V = L × W^2/2$.

#### 2.11.3. Subcutaneous xenograft ATRA-resistant APL model

To establish the subcutaneous xenograft ATRA-resistant APL model, NB4-R2 cells (5 × 10^6) were subcutaneously injected into the male BALB/C nude mice (GemPharmatech, China) at 4-5-week-old. ATRA (20 mg/kg, ip) or GRh2 (20 mg/kg, ig) was injected every alternate day when the tumor volume reached approximately 100–200 mm^3. After 20 days of treatment, the mice were euthanized. The spleen was examined using HE staining to detect APL cell infiltration. The tumor was assessed using IHC to detect METTL3 expression.

2.12. Molecular docking validation

Download the protein structure of METTL3 (PDB ID: 5IL0) from the RCSB PDB database and import it into Autodock (v1.5.6). The MDL Molfile format of GRh2 was obtained from the pubchem database and imported into ChemBio3D Ultra 14.0 software for energy minimization. POCASA 1.1 was used to predict the protein binding site, Autodock4.26 was used for docking, and PyMOL 2.3.0 and LigPlotV 2.2.5 were used to analyze the interaction mode of the docking results.

2.13. Data analysis

The data is presented as mean ± standard deviation. Statistical analyses were performed using GraphPad Prism 9. The differences between two groups were determined by an independent sample Student's t-test, and a one-way analysis of variance (ANOVA) was used for multiple group comparisons. Differences were considered statistically significant
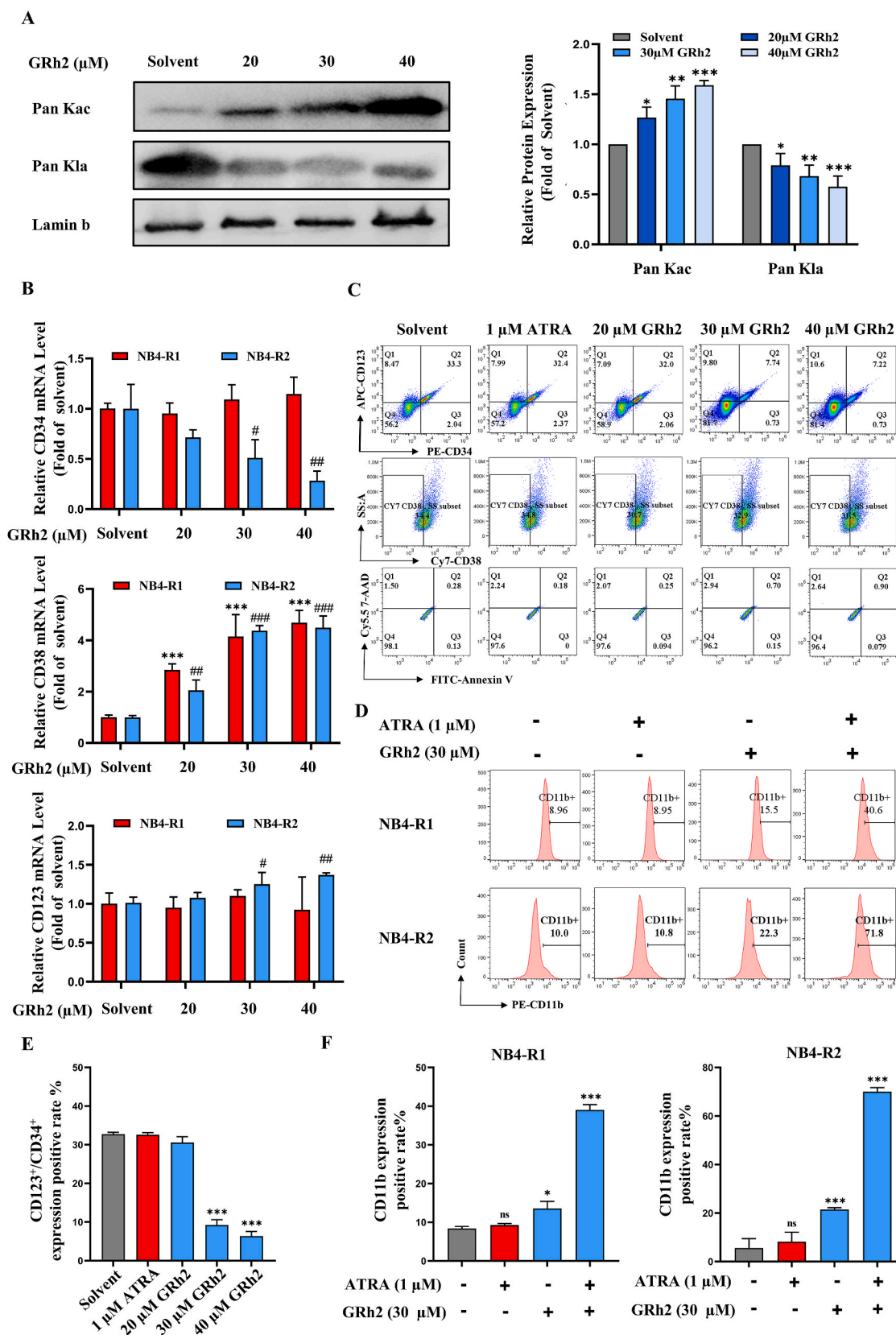
Fig. 2. GRh2 acted similarly to histone lactylation inhibitors

(A) Detection of Pan kac and Pan kla expression levels in NB4-R2 cell treated with 0–40 μM GRh2 for 48 h by Western blot analysis. (n = 3, *P < 0.05, **P < 0.01, ***P < 0.001 versus solvent). (B) The expression level of CD34, CD38 and CD123 in NB4-R1 and NB4-R2 cells treated with 0–40 μM GRh2 for 48 h was detected via qRT-PCR. (n = 3, ***P < 0.001 versus NB4-R1; #P < 0.05, ##P < 0.01, ###P < 0.001 versus NB4-R2). (C, E) The apoptosis rates of ATRA-resistance LSCs labeled with CD34+CD38−CD123+ in NB4-R2 cell treated with 0–40 μM GRh2 for 48 h were detected by FCM. (n = 3, ***P < 0.001 versus solvent) (D, F) FCM were used to detect CD11b+ cell ratios in NB4-R1 and NB4-R2 cells treated with 30 μM GRh2 and 1 μM ATRA for 48 h (n = 3, *P < 0.05, ***P < 0.001).
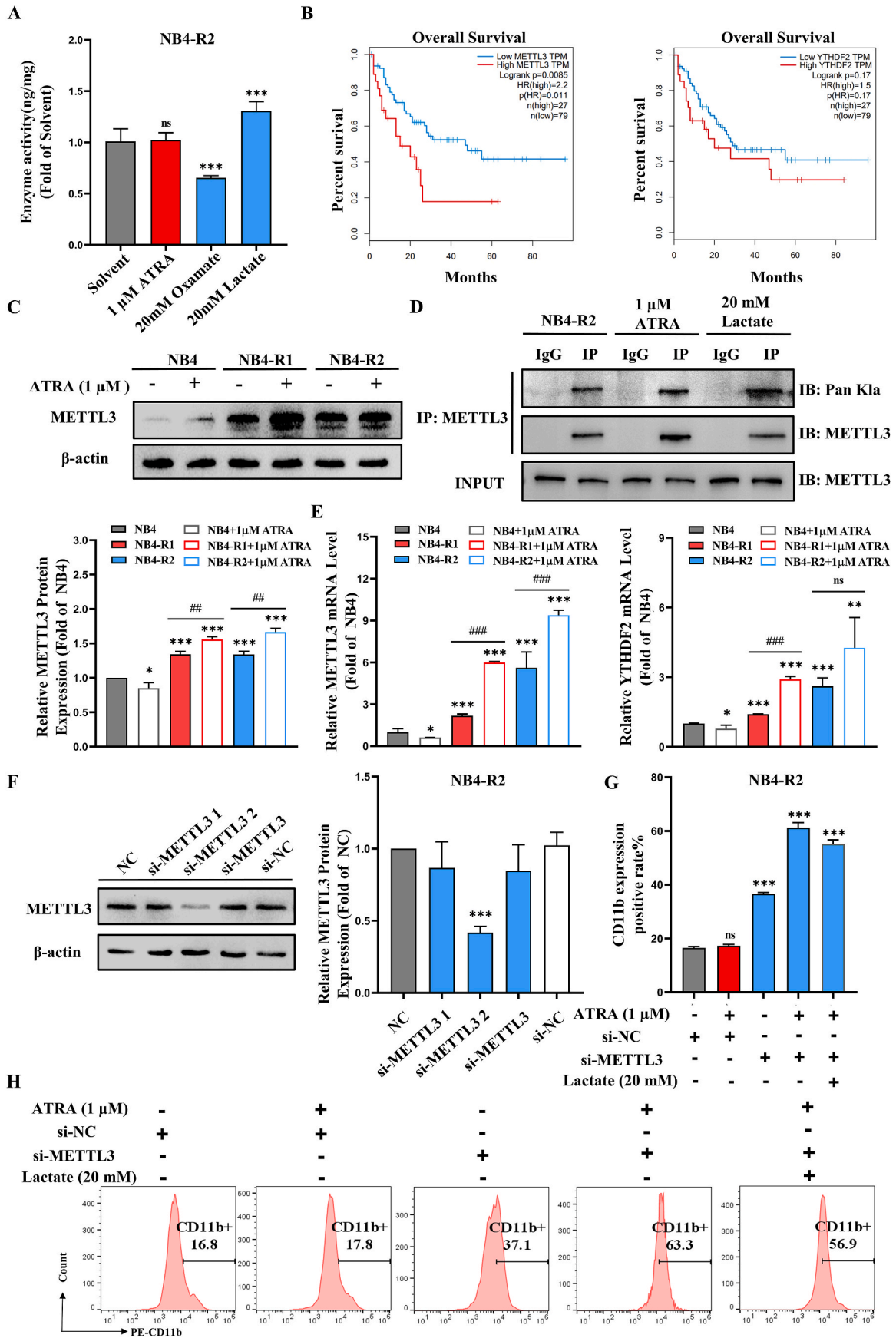
(caption on next page)

Fig. 3. Lactate induced upregulation of METTL3 in ATRA-resistant APL Cells

(A) Detection of specific m^{6}A epigenetic methylation enzyme activity in NB4-R2 cell treated with 20 μM oxamate or 20 μM lactate or 1 μM ATRA for 48 h (n = 3, ***P < 0.001 versus solvent) (B) Kaplan-Meier analysis using the GEPIA website to correlate expression levels of METTL3 and YTHDF2 with survival prognosis in AML. (C) Detection of METTL3 expression levels in NB4, NB4-R1 and NB4-R2 cells treated with 1 μM ATRA for 48 h by Western blot analysis. (n = 3, *P < 0.05, **P < 0.01, ***P < 0.001 versus NB4; ##P < 0.01, ###P < 0.001). (D) Detection of Pan kla expression level on METTL3 after the treatment of 1 μM ATRA or 20 μM lactate for 48 h in NB4-R2 cell using CO-IP. (E) qRT-PCR was used to detect the expression level of METTL3 in NB4, treated with 1 μM ATRA for 48 h (n = 3, *P < 0.05, ***P < 0.001 versus NB4; ##P < 0.01). (F) NB4-R2 cell were transfected with si-METTL3 for 48 h. METTL3 expression levels were determined by western blotting. (n = 3, ***P < 0.001 versus NC). (G, H) FCM were used to detect CD11b$^+$ cell ratios in NB4-R2 cells transfected with si-METTL3 and treated with 1 μM ATRA for 48 h (n = 3, ***P < 0.001).

at *P < 0.05, **P < 0.01, ***P < 0.001; #P < 0.05, ##P < 0.01, ###P < 0.001.

3. Results

3.1. Histone lactylation levels increased in ATRA-resistance APL cells

To uncover the molecular mechanisms behind ATRA resistance in APL, we obtained the ATRA-sensitive APL cell line (NB4) and ATRA-resistant APL cell lines (NB4-R1, NB4-R2). We conducted NBT and FCM to assess the level of cell differentiation [11]. Our results indicated that the ATRA-resistant APL cells exhibit reduced sensitivity to ATRA differentiation treatment (Supplementary Figs. 1A–D).

Lactate as a precursor molecule accumulated during metabolism enhances clinical drug resistance by modulating histone lactylation and acetylation [12,13]. Our data revealed that the levels of lactate dehydrogenase (LDH) and lactate in ATRA-resistant APL cells was elevated (Fig. 1A). ATRA induces APL cells differentiation by promoting the degradation of PML-RARα oncoprotein [14]. The resistance of NB4-R2 is related to mutations in the ligand-binding portion of the intracellular PML-RARα fusion protein. For further research, we employed RNA-seq analysis to screen differentially expressed genes between the ATRA-sensitive APL cell line NB4 and the ATRA-resistant APL cell line NB4-R2. Kyoto Encyclopedia of Genes and Genomes (KEGG) analysis highlighted significant differences in Lactic acid metabolism pathway (Fig. 1B). Western blotting analysis showed an increase in the levels of Pan-lysine lactylation (Pan Kla) and H3K18la levels in ATRA-resistant APL cells, and this was further enhanced after a 48h intervention with 1 μM ATRA (Fig. 1C). Compared with NB4-R1, the up-regulation of Pan kla was much more remarkable in NB4-R2. Therefore, we chose NB4-R2 for subsequent experiments.

LSCs and ATRA-resistant APL cells are the primary culprits behind leukemia recurrence after remission [15]. We used flow cytometry to detect cell populations with cell phenotypes of CD34$^+$, CD38$^-$, CD123$^+$ in NB4-R2 cell line and identified them as ATRA-resistance LSCs [16, 17]. To further evaluate the role of histone lactylation inhibitor in ATRA-resistance APL, we used oxamate to reduce the overall intracellular histone lactylation level in NB4-R2 cells (Supplementary Fig. 1E). After a 48h treatment, our results showed that the treatment of oxamate considerably reduced histone lactylation and promoted apoptosis of ATRA-resistance LSCs (Fig. 1D, F). Oxamate also enhanced the sensitivity of NB2-R1 and R2 cells to ATRA treatment in cell differentiation (Fig. 1E, G).

3.2. GRh2 acted similarly to histone lactylation inhibitor

GRh2 is reported as an effective natural histone deacetylase inhibitor. It suppressed the proliferation and inducing apoptosis in CML and M3 type of AML cells via increasing histone acetylation level [10]. However, whether GRh2 modulate histone acetylation and lactylation in ATRA-resistant APL cells remains unknown. First, GRh2 was selected for

the following study (Supplementary Fig. 1F). We then examined the effect of GRh2 for 48h on histone acetylation and lactylation levels in ATRA-resistant APL cells. Our results showed that the level of overall histone acetylation increased and histone lactylation decreased compared to ATRA-sensitive APL cell line NB4 (Fig. 2A). GRh2 considerably reduced mRNA expression of CD34 in NB4-R2, while upregulating the mRNA level of CD123. The mRNA levels of CD38 were significantly elevated in both NB4-R1 and NB4-R2 in a dose-dependent manner (Fig. 2B). FCM results showed that GRh2 did not significantly promote the apoptosis of ATRA-resistant LSCs, but inhibited the positive expression of CD34/CD123. (Fig. 2C, E). GRh2 increased APL sensitivity to ATRA treatment in ATRA-resistant cells (Fig. 2D, F). These data suggested that GRh2 acted similarly to histone lactylation inhibitors.

3.3. Lactate induced upregulation of METTL3 in ATRA-resistant APL cells

Methylation at the adenosine N^6 location (m^{6}A) is the most abundant modification on mRNA and noncoding RNA. Recent studies have shown that METTL3 is a core RNA methyltransferase that catalyzes the formation of m^{6}A [18]. Lactylation has been proven to drive METTL3 mediated RNA m^{6}A modification [19,20]. Using a specific m^{6}A epigenetic methylation enzyme activity detection kit, we found that lactate considerably affected m^{6}A enzyme activity in ATRA-resistant APL cells (Fig. 3A). YTHDF2 is a m^{6}A reader known to promote AML progression [21]. Kaplan-Meier analysis from the GEPIA website revealed that high expression of METTL3 was associated with poor survival in AML. Although there is no significant difference, it can be seen from the available data that the survival rate of AML patients with high expression of YTHDF2 is relatively shorter.(Fig. 3B). Further, western blotting analysis showed significant upregulation of METTL3 expression in ATRA-resistant APL cells, with a further increase observed after a 1 μM ATRA intervention for 48h (Fig. 3C). Co-IP results showed the increased level of lactylation on METTL3 after the treatment of ATRA or exogenous lactate (Fig. 3D). We then found the increased mRNA expression of METTL3 and YTHDF2 in ATRA-resistant APL cells (Fig. 3E). Notably, compared to the NB4-R1 cell line, NB4-R2 exhibited a more significant increase in lactylation levels and METTL3 expression. Therefore, we chose NB4-R2 for subsequent experiments.

To further established the effect of METTL3 in ATRA-resistant APL, METTL3 expression levels were decreased in NB4-R2 cells with si-METTL3 transfection (Fig. 3F). si-METTL3 resisted the ATRA differentiation (Fig. 3G and H). These findings suggested that high expression of METTL3 driven by lactylation modifications promotes ATRA-resistance in APL.

3.4. Correlation between METTL3 and ATRA-resistance in mice with APL xenograft tumors

To validate whether the overexpression of METTL3 in APL cells promotes ATRA resistance in vivo, we established two xenografted APL
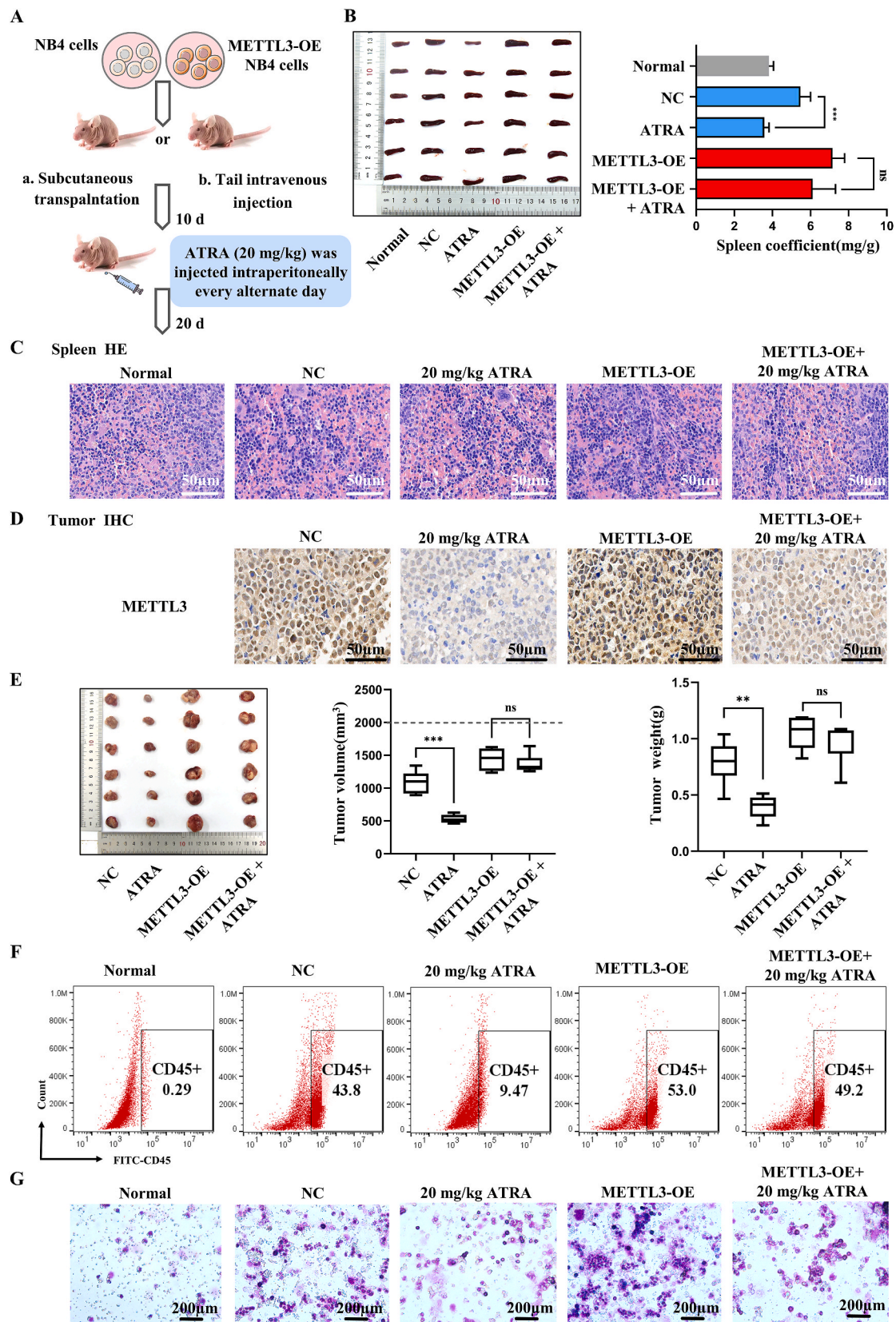
Fig. 4. Correlation between METTL3 and ATRA-resistance in mice with APL xenograft tumors

(A) APL xenograft tumor mouse model establishment flowchart, including subcutaneous injection and tail vein injection methods. (B) Spleen images and spleen coefficient. (n = 6, ***P < 0.001). (C) Spleen HE images. (D) METTL3 IHC staining in tumor tissues. (E) Tumor images, tumor volume and tumor weight. (n = 6, **P < 0.01, ***P < 0.001). (F) FCM were used to detect CD45$^+$ cell ratios in the bone marrow. (G) Wright-Giemsa were used to detect APL load.
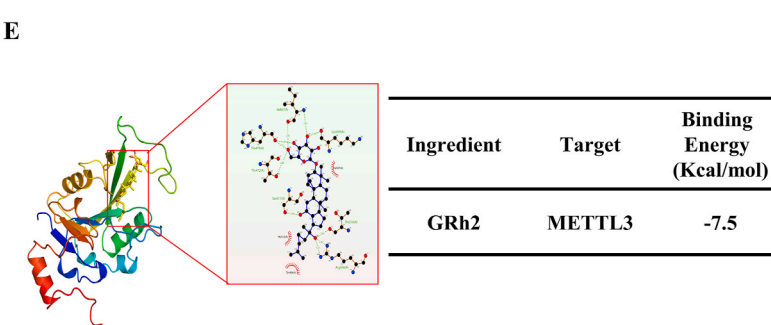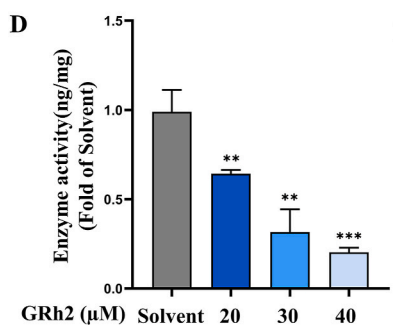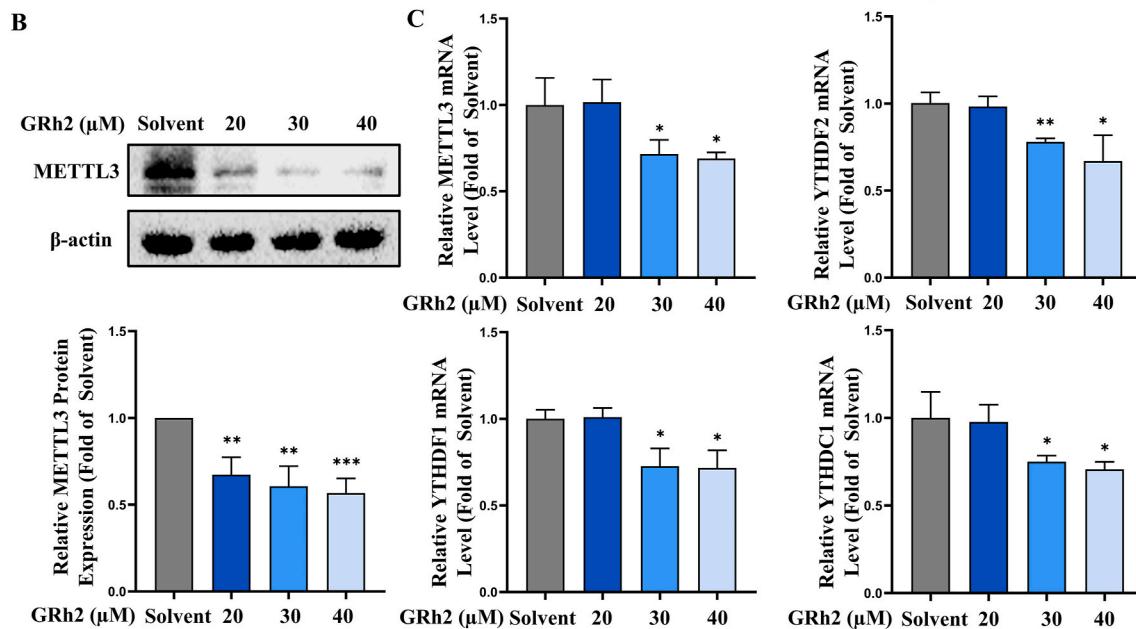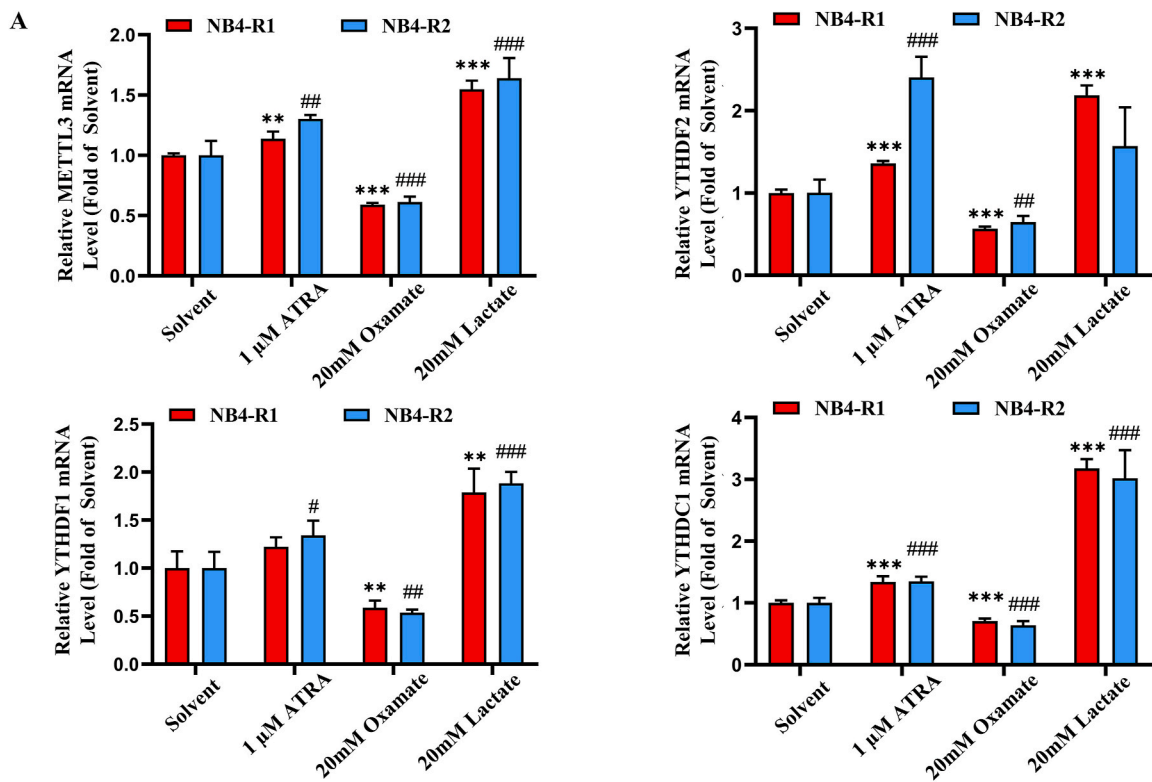
(caption on next page)

Fig. 5. GRh2 inhibited METTL3 in ATRA-resistant APL cells
(A) The expression level of METTL3, YTHDF1, YTHDF2, and YTHDC1 in NB4-R1 and NB4-R2 cells treated with 20 μM oxamate or 20 μM lactate or 1 μM ATRA for 48 h was detected via qRT-PCR. (n = 3, **P < 0.01, ***P < 0.001 versus NB4-R1; ##P < 0.01, ###P < 0.001 versus NB4-R2). (B) Detection of METTL3 expression levels in NB4-R2 cell treated with 0–40 μM GRh2 for 48 h by Western blot analysis. (n = 3, **P < 0.01, ***P < 0.001 versus solvent). (C) The expression level of METTL3, YTHDF1, YTHDF2, and YTHDC1 in NB4-R2 cell treated with 0–40 μM GRh2 for 48 h was detected via qRT-PCR. (n = 3, *P < 0.05, **P < 0.01 versus solvent). (D) Detection of specific m^6A epigenetic methylation enzyme activity in NB4-R2 cell treated with 0–40 μM GRh2 for 48 h (n = 3, **P < 0.01, ***P < 0.001 versus solvent). (E) Molecular docking results of GRh2 with METTL3.

mouse models (Fig. 4A). NB4 cells transfected with METTL3-OE were transplanted into BALB/C nude mice via tail vein injection and subcutaneously inoculation. 20 mg/kg ATRA was injected intraperitoneally every alternate day after tumor formation. The weight and volume of tumors and spleen coefficients are marks in mice with APL xenograft tumors [22,23]. The size of spleens in tail vein injected APL model group were notably increased (Fig. 4B). ATRA treatment improved splenic lesions, but the overexpression of METTL3 diminished the therapeutic effect of ATRA (Fig. 4C). Tumor IHC analysis showed the upregulated expression level of METTL3, in the METTL3-OE group (Fig. 4D). The weight and volume of tumors have not been improved in the METTL3-OE group compared with the ATRA group (Fig. 4E).

CD45$^+$ and Giemsa staining were used to analyze the number of leukemia cells in the bone marrow [24]. In subcutaneous inoculated model, our results showed that the counts of CD45$^+$ leukemia cells and Giemsa positive cells increase in the METTL3-OE group (Fig. 4F and G). These results suggested that METTL3 promotes ATRA-resistance in APL.

3.5. GRh2 inhibited METTL3 in ATRA-resistant APL cells

Our results showed that histone lactylation inhibitor considerably inhibited mRNA expression of MEETL3 and its downstream reading protein YTHDF2, YTHDF1 and YTHDC1 (Fig. 5A). Considering that GRh2 inhibits histone lactylation, we speculated whether GRh2 could inhibit the function of METTL3. Our results showed that GRh2 dose-dependently inhibits the expression level of METTL3 (Fig. 5B) and its downstream reading protein YTHDF2, YTHDF1 and YTHDC1 (Fig. 5C). Results in specific m^6A epigenetic methyltransferase activity detection showed that GRh2 dose-dependently inhibited the enzyme activity of METTL3 (Fig. 5D). Molecular docking also revealed that GRh2 has a high directly affinity to METTL3 (Fig. 5E).

3.6. GRh2 suppressed METTL3 expression and enhanced the sensitivity to ATRA differentiation therapy in mice with ATRA-resistant APL xenograft tumors

We then elevated the effect of GRh2 in mice with ATRA-resistant APL xenograft tumors. NB4-R2 cells were inoculated subcutaneously into the BALB/C nude mice. After 10 days, both ATRA and GRh2 were injected every alternate day (Fig. 6A). Survival curve showed that GRh2 treatment considerably elevated the survival of ATRA-resistant APL xenograft mice (Fig. 6B). ATRA treatment showed no effect on the splenic lesions in ATRA-resistant APL model group. GRh2 enhanced the therapeutic effect of ATRA (Fig. 6C and D). Tumor IHC revealed that GRh2 considerably inhibited the expression of METTL3 (Fig. 6E). The tumor volume and weight also decreased considerably in GRh2 and ATRA combination group (Fig. 6F). In conclusion, these results suggested that GRh2 could inhibit the expression and function of METTL3. GRh2 also enhanced the sensitivity of APL cells to ATRA differentiation therapy, further supporting METTL3 as a promising therapeutic target for ATRA-resistant APL.

4. Discussion

ATRA is a first-line drug for treating APL. Clinical studies have shown

that APL patients receiving ATRA has a high bone marrow complete remission (CR) rate (94 %) [25]. However, ATRA-resistance in APL patients severely limits its efficacy and is a key reason for poor prognosis [3].

High concentrations of lactic acid in tumor cells induce histone lactylation, and previous studies have revealed that high expression of lactylation play a role in the regulation of anti-tumor drug resistance [26,27]. We found that lactate accumulation in ATRA-resistant APL cells regulates its lactylation modification level, and targeting to histone lactylation effectively inhibits ATRA-resistance.

The balance between histone lactylation and acetylation is determined by the synergistic levels of lactate and acetyl-CoA [28]. Ginseng has been used in traditional Chinese medicine for thousands of years and has been demonstrated as an effective natural histone deacetylase to promote the CML and M3 type of AML cells apoptosis [10]. However, the association between GRh2, lactylation and acetylation in ATRA-resistance APL has not been mentioned. We first proved that GRh2 increases histone acetylation levels and considerably inhibits the lactylation level in ATRA-resistant APL cells. Furthermore, GRh2 enhanced sensitivity of ATRA differentiation therapy and promoted apoptosis of ATRA-resistance LSCs, suggesting that GRh2 acts similarly to lactylation inhibitors.

METTL3 is m^6A methyltransferase, which functions in RNA methylation, affecting gene expression and is associated with tumor development. During the preparation of the manuscript, Li et al. reported the identification of a new AML chemotherapy resistance protein METTL3, which can mediate AML cell homing via m^6A [29]. In addition, Lactylation has been proven to drive METTL3 mediated RNA m^6A modification to promote the immunosuppression of tumor-infiltrating bone marrow cells [19]. We hypothesized that lactic acid-driven lactylation modification could enhance METTL3 expression in ATRA-resistant APL.

Withing a specific m^6A epigenetic methylation enzyme activity detection kit, we found that lactate considerably affected the enzyme activity of METTL3 in ATRA-resistant APL cells. Co-IP showed that there are lactylation sites on METTL3 in ATRA-resistant APL cells, and the intervention of ATRA and exogenous lactate further enhanced the lactylation modification on METTL3. Additionally, in mice with APL xenograft tumors, overexpression of METTL3 promoted tumor growth and increased ATRA resistance in APL.

Next, we studied the relationship between GRh2 and METTL3 in the lactylation-mediated pathway. Our data showed that GRh2 considerably inhibits METTL3 expression in ATRA-resistant APL cells in a concentration-dependent manner. In addition, molecular docking results suggested that GRh2 bind well with METTL3 directly. Consistent with the in vitro antileukemic effect, studies have shown that in the mice with ATRA-resistant APL xenograft tumors, GRh2 considerably reduced tumor weight and volume and suppressed tumor METTL3 expression.

5. Conclusion

Upregulation of METTL3 driven by lactylation modifications promotes ATRA resistance in APL. GRh2 could act as a potential inhibitor for lactylation-driven METTL3 to ameliorates ATRA resistance in APL.
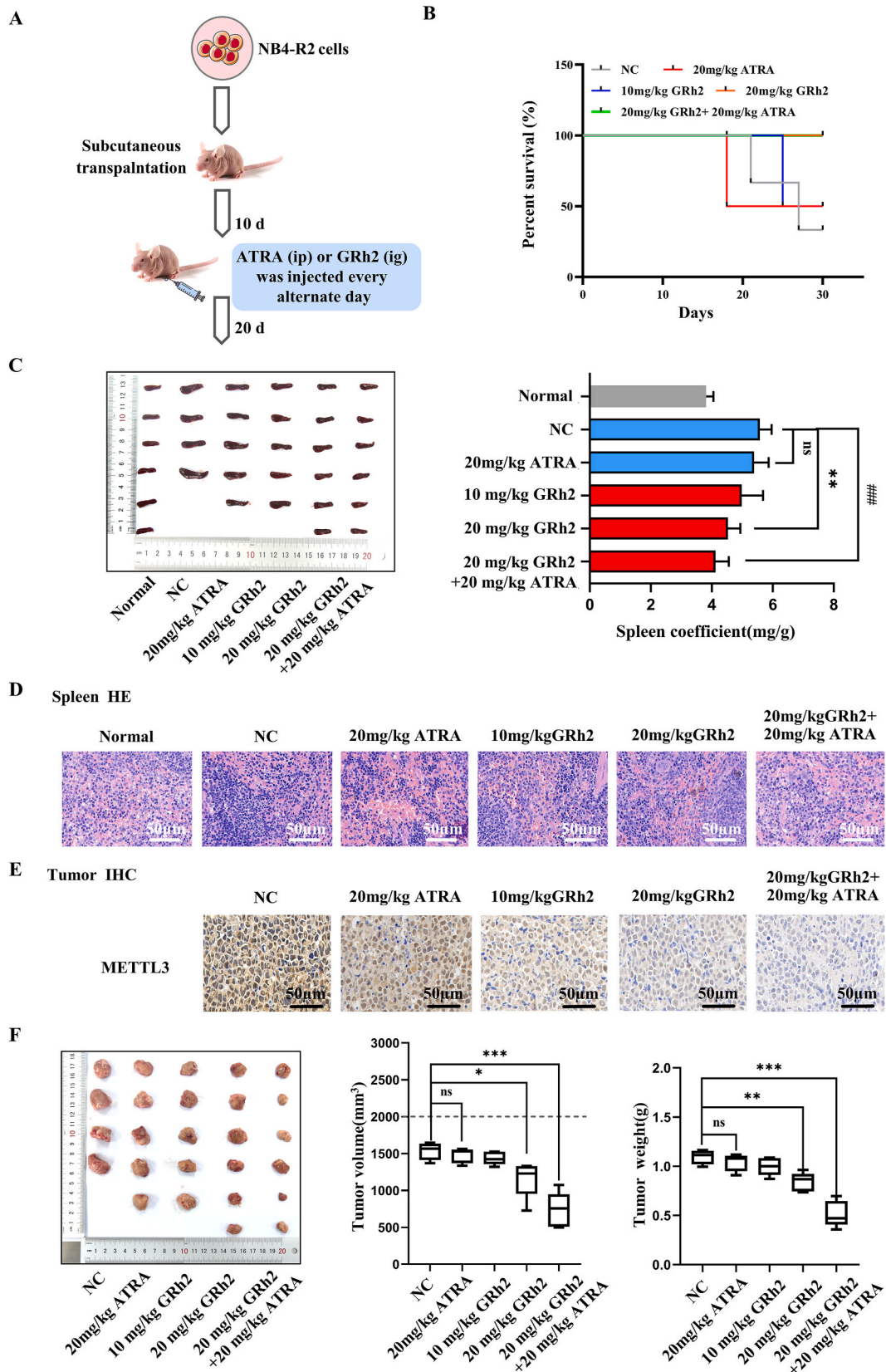
Fig. 6. GRh2 suppressed METTL3 expression and enhanced the sensitivity to ATRA differentiation therapy in mice with ATRA-resistant APL xenograft tumors (A) ATRA-resistant APL xenograft mouse model establishment flowchart. (B) Recording of survival rate (%) with Kaplan-Meier curve plots. (C) Spleen images and spleen coefficient. (n = 6, **P < 0.01; ###P < 0.001). (D) Spleen HE images. (E) METTL3 IHC staining in tumor tissues. (F) Tumor images, tumor volume and tumor weight. (n = 6, *P < 0.05; **P < 0.01; ***P < 0.001).

Declaration of competing interest

The authors declare that they have no known competing financial interests or personal relationships that could have appeared to influence the work reported in this paper.

Acknowledgments

Appendix A. Supplementary data

Supplementary data to this article can be found online at https://doi.org/10.1016/j.jgr.2023.12.003.

References

[1] Yilmaz M, Kantarjian H, Ravandi F. Acute promyelocytic leukemia current treatment algorithms. Blood Cancer J 2021;6:123.
[2] Huang ME, Ye YC, Chen SR, Chai JR, Lu JX, Zhoa L, et al. Use of all-trans retinoic acid in the treatment of acute promyelocytic leukemia. Blood 1988;2:567–72.
[3] Gallagher RE. Retinoic acid resistance in acute promyelocytic leukemia. Leukemia 2002;10:1940–58.
[4] Baysal M, Gürsoy V, Hunutlu FC, Erkan B, Demirci U, Bas V, et al. The evaluation of risk factors leading to early deaths in patients with acute promyelocytic leukemia: a retrospective study. Ann Hematol 2022;5:1049–57.
[5] Brand A, Singer K, Koehl GE, Kolitzus M, Schoenhammer G, Thiel A, et al. LDHA-associated lactic acid production blunts tumor immunosurveillance by T and NK cells. Cell Metabol 2016;5:657–71.
[6] Zhang D, Tang Z, Huang H, Zhou G, Cui C, Weng Y, et al. Metabolic regulation of gene expression by histone lactylation. Nature 2019;7779:575–80.
[7] Dai B, Wang F, Wang Y, Zhu J, Li Y, Zhang T, et al. Targeting HDAC3 to overcome the resistance to ATRA or arsenic in acute promyelocytic leukemia through ubiquitination and degradation of PML-RARα. Cell Death Differ 2023;5:1320–33.
[8] Noack K, Mahendrarajah N, Hennig D, Schmidt L, Grebien F, Hildebrand D, et al. Analysis of the interplay between all-trans retinoic acid and histone deacetylase inhibitors in leukemic cells. Arch Toxicol 2017;5:2191–208.
[9] Zhu S, Liu X, Xue M, Li Y, Cai D, Wang S, et al. 20(S)-ginsenoside Rh2 induces caspase-dependent promyelocytic leukemia-retinoic acid receptor A degradation in NB4 cells via Akt/Bax/caspase9 and TNF-α/caspase8 signaling cascades. J Ginseng Res 2021;2:295–304.
[10] Liu Z-H, Li J, Xia J, Jiang R, Zuo G-W, Li X-P, et al. Ginsenoside 20(s)-Rh2 as potent natural histone deacetylase inhibitors suppressing the growth of human leukemia cells. Chem Biol Interact 2015:227–34.
[11] Zhang SY, Zhu J, Chen GQ, Du XX, Lu LJ, Zhang Z, et al. Establishment of a human acute promyelocytic leukemia-ascites model in SCID mice. Blood 1996;8:3404–9.
[12] Li W, Zhou C, Yu L, Hou Z, Liu H, Kong L, et al. Tumor-derived lactate promotes resistance to bevacizumab treatment by facilitating autophagy enhancer protein RUBCNL expression through histone H3 lysine 18 lactylation (H3K18la) in colorectal cancer. Autophagy 2024;20(1):114–30.
[13] Wagner W, Ciszewski WM, Kania KD. L- and D-lactate enhance DNA repair and modulate the resistance of cervical carcinoma cells to anticancer drugs via histone deacetylase inhibition and hydroxycarboxylic acid receptor 1 activation. Cell Commun Signal 2015;36.
[14] Tomita A, Kiyoi H, Naoe T. Mechanisms of action and resistance to all-trans retinoic acid (ATRA) and arsenic trioxide (As2O 3) in acute promyelocytic leukemia. Int J Hematol 2013;6:717–25.
[15] van Rhenen A, Feller N, Kelder A, Westra AH, Rombouts E, Zweegman S, et al. High stem cell frequency in acute myeloid leukemia at diagnosis predicts high minimal residual disease and poor survival. Clin Cancer Res 2005;18:6520–7.
[16] Xie W, Wang X, Du W, Liu W, Qin X, Huang S. Detection of molecular targets on the surface of CD34+CD38- bone marrow cells in myelodysplastic syndromes. Cytometry 2010;9:840–8.
[17] Kandeel EZ, El Sharkawy N, Hanafi M, Samra M, Kamel A. Tracing leukemia stem cells and their influence on clinical course of adult acute myeloid leukemia. Clin Lymphoma, Myeloma & Leukemia 2020;6:383–93.
[18] Zeng C, Huang W, Li Y, Weng H. Roles of METTL3 in cancer: mechanisms and therapeutic targeting. J Hematol Oncol 2020;1:117.
[19] Xiong J, He J, Zhu J, Pan J, Liao W, Ye H, et al. Lactylation-driven METTL3-mediated RNA m6A modification promotes immunosuppression of tumor-infiltrating myeloid cells. Mol Cell 2022;9.
[20] Zhang L, Wang X, Che W, Zhou S, Feng Y. METTL3 silenced inhibited the ferroptosis development via regulating the TFRC levels in the Intracerebral hemorrhage progression. Brain Res 2023:148373.
[21] Zhang Z, Zhou K, Han L, Small A, Xue J, Huang H, et al. RNA m6A reader YTHDF2 facilitates precursor miR-126 maturation to promote acute myeloid leukemia progression. Genes Dis 2023;1:382–96.
[22] Jiang W, Hu Y, Wang X, Zhang Q, Guo X, Cheng S, et al. miR-125b-5p-MAPK1-C/EBPα feedback loop regulates all-trans retinoic acid resistance in acute promyelocytic leukemia. Gene 2023:147806.
[23] Tong Q, You H, Chen X, Wang K, Sun W, Pei Y, et al. ZYH005, a novel DNA intercalator, overcomes all-trans retinoic acid resistance in acute promyelocytic leukemia. Nucleic Acids Res 2018;7:3284–97.
[24] Shao X, Chen Y, Wang W, Du W, Zhang X, Cai M, et al. Blockade of deubiquitinase YOD1 degrades oncogenic PML/RARα and eradicates acute promyelocytic leukemia cells. Acta Pharm Sin B 2022;4:1856–70.
[25] Chen ZX, Xue YQ, Zhang R, Tao RF, Xia XM, Li C, et al. A clinical and experimental study on all-trans retinoic acid-treated acute promyelocytic leukemia patients. Blood 1991;6:1413–9.
[26] He Y, Ji Z, Gong Y, Fan L, Xu P, Chen X, et al. Numb/Parkin-directed mitochondrial fitness governs cancer cell fate via metabolic regulation of histone lactylation. Cell Rep 2023;2:112033.
[27] Sun X, He L, Liu H, Thorne RF, Zeng T, Liu L, et al. The diapause-like colorectal cancer cells induced by SMC4 attenuation are characterized by low proliferation and chemotherapy insensitivity. Cell Metabol 2023;9.
[28] Dai X, Lv X, Thompson EW, Ostrikov KK. Histone lactylation: epigenetic mark of glycolytic switch. Trends Genet 2022;2:124–7.
[29] Li M, Ye J, Xia Y, Li M, Li G, Hu X, et al. METTL3 mediates chemoresistance by enhancing AML homing and engraftment via ITGA4. Leukemia 2022;11:2586–95.